Journal of
Water & Climate Change

Check for updates

IWA PUBLISHING

© 2022 The Authors

Journal of Water and Climate Change Vol 13 No 9, 3416 doi: 10.2166/wcc.2022.153

Quantifying the changes in the runoff and its components across the Upper Indus River Basin under climate change

Sohaib Baig*, Takahiro Sayama and Masafumi Yamada

Disaster Prevention Research Institute, Kyoto University, Gokasho, Uji, Kyoto 611-0011, Japan
*Corresponding author. E-mail: baig.sohaib.2 s@kyoto-u.ac.jp; aquarius_baig@yahoo.com

ABSTRACT

The runoff from the Upper Indus River Basin (UIB) is considered vital for sustainable water supply and agriculture. Climate change may alter the runoff and affect the availability of water. This study employs a hydrologic model and the climate projections of fine-resolution Meteorological Research Institute-Atmospheric General Circulation Model (MRI-AGCM) (0.1875°) to assess the impacts of climate change in the future (2075–2099) on the flows in the UIB and its sub-basins. The simulations have shown satisfactory results compared to the observed ones. Furthermore, simulated snow-cover was compared with estimated snow-cover by Moderate Resolution Imaging Spectroradiometer (MODIS). According to the results, meltwater from glaciers contributes to about two-thirds of the annual runoff from the UIB. According to the projections, the future temperature will increase by 5.3 °C and annual precipitation will increase by 17% across the UIB. Despite this increase, the annual river flows were projected to decrease by 14% in the future because of depleted glacier melt. Furthermore, the detailed hydrologic responses in selected sub-basins showed different patterns in the future depending on the climate and elevation. In an eastern sub-basin, flows will increase by 58% because of enhanced glacier melt and higher precipitation. Contrarily, two western sub-basins will experience the reduction of the flow by 30–70% because of the glacier retreat.

Key words: Bisham Qila, climate change, hydrology, Pakistan, river flows, Upper Indus Basin

HIGHLIGHTS

- Runoff in the Upper Indus River Basin (UIB) is melt-dependent.
- The precipitation regime in the east is monsoon dominated while in the west it is snowfall dependent.
- Hydrologic response across the UIB is contrasting because of climate and geography.
- Owing to the fine resolution of the MRI-AGCM, distinct climatic features across the UIB have been projected.
- Climate change and glacier retreat will alter the quantity and timings of the hydrographs in the future.

ABBREVIATIONS

APHRODITE	Asian Precipitation Highly Resolved Observational Data Integration Towards Evaluation
GCM	General Circulation Model
ICIMOD	International Centre for Integrated Mountain Development
MODIS	Moderate Resolution Imaging Spectroradiometer
MRI-AGCM	Meteorological Research Institute-Atmospheric General Circulation Model
RCM	Regional Climate Model
RCP	Representative concentrative pathway
RRI	Rainfall–runoff–inundation
UIB	Upper Indus River Basin

1. INTRODUCTION

The Indus River Basin covers an area of 1,140,000 km^2 in Afghanistan, China, India, and Pakistan. The length of the river is approximately 2,800 km, and its origin lies in Tibet (Figure 1) (Ali 2013). The Upper Indus River Basin (UIB) supplies river flows that are essential for one of the world's largest contiguous canal irrigation systems (Lutz *et al.* 2016).

This is an Open Access article distributed under the terms of the Creative Commons Attribution Licence (CC BY 4.0), which permits copying, adaptation and redistribution, provided the original work is properly cited (http://creativecommons.org/licenses/by/4.0/).

Downloaded from http://iwaponline.com/jwcc/article-pdf/13/9/3416/1114580/jwc0133416.pdf
by KYOTO UNIVERSITY user

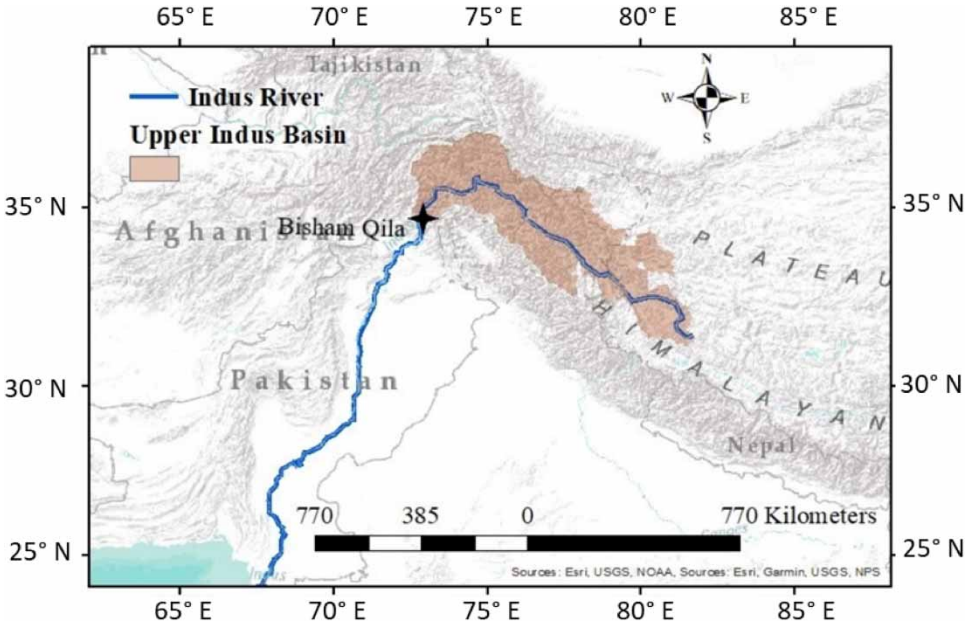

Figure 1 | Map of the UIB with its outlet at Bisham Qila.

Climate in the UIB is quite variable, in winter (October to March) temperatures often remain sub-freezing where average temperature remains around 9 °C, while the average temperature in summer (May–September) is approximately 13 °C (Mcsweeney *et al.* 2012). Reggiani & Rientjes (2015) used the mass-balance technique and estimated the total annual precipitation in the basin to be 681 ± 100 mm. Similar estimates of total annual precipitation have been reported by Dahri *et al.* (2018) and Immerzeel *et al.* (2015). In winter, precipitation falls as snow which accumulates in the season and melts in spring; this meltwater from snow and glaciers results in higher flows from July to September (Archer 2003; Mukhopadhyay & Khan 2014). At the downstream of Bisham Qila, the Tarbela Reservoir supplies water essential for irrigation, stores flood water, and generates hydropower (Figure 1) (Lutz *et al.* 2016).

The hydrological cycle of the UIB is under stress because of climate change. Rising temperatures will cause more water to evaporate, which will increase the moisture content in the atmosphere and render the spatiotemporal trends in precipitation more variable (Wester *et al.* 2019). In addition to precipitation variability, the increased temperature will alter the hydrological cycle in the UIB (Immerzeel *et al.* 2010). The topographic features and climate vary across the UIB which controls the hydrologic cycle. There is a need to explore the hydrology at sub-basins in the UIB to understand the shift in the quantity and timings of the runoff under the future climate. Future climate change in the Himalayan–Karakoram region, where the UIB is located, has been projected by Sanjay *et al.* (2017) using the dynamic downscaling of Regional Climate Models (RCMs). According to these projections, temperatures will increase between 2.4 and 3.6 °C by the mid-century scenario and between 3.0 and 5.0 °C by the end of this century. The annual precipitation will increase in the range of 3.5–12.8% in the mid- and late centuries in the region. The two studies that employed a fine-resolution General Circulation Model (GCM) (~25 km) and the latest CMIP6 have projected wetter summers in the UIB in the future (Ali *et al.* 2021; Abbas *et al.* 2022). Glaciers in the region will not be able to retain their mass despite the increase in precipitation because the increase in temperatures will make the current mass balance negative (Lutz *et al.* 2016). This situation will result in an increase in glacier melt rates in the coming decades until the last quarter of this century (Rounce *et al.* 2020).

The hydrologic analysis in UIB has used various techniques and datasets. Often global datasets are employed owing to the unavailability of the *in situ* data. Lutz *et al.* (2016) and Su *et al.* (2016) included glacier mass-balance modeling in the hydrologic analysis to evaluate the impacts of climate change in the UIB and its sub-basins. The simulations demonstrated the contribution of glaciers along with snow and rainfall which helped in understanding the seasonal changes in the stream flow discharge. Ougahi *et al.* (2022) and Shah *et al.* (2020) used GCMs to project the river flows in the UIB using the SWAT hydrologic model. They have projected that river flows will increase in the mid- and late century, although the rate

Downloaded from http://iwaponline.com/jwcc/article-pdf/13/9/3416/1114580/jwc0133416.pdf
by KYOTO UNIVERSITY user

of increase will be milder in the later century. Higher increases are projected in the spring and summer because of earlier snow melt and precipitation. Kiani *et al.* (2021) focused on the temperature increase of 1.5–2 °C as the critical threshold in the UIB. Under both the threshold scenarios, the annual river flows are projected to increase in the range of 11–26% because of the earlier onset of snow and glacier melt. Similar temperature thresholds were used by Hasson *et al.* (2019) to evaluate the hydrologic response in the UIB. However, their modeling approach uses a variety of glacier coverage scenarios ranging from 0 to 100%. Their simulations show that annual river flows will increase in the case of the intact glacier while decreasing in all other glacier coverage scenarios. Ali *et al.* (2021) used two finer resolution climate models in the UIB, the results suggested that river flows will continue to increase in the mid-century (50–60%) and late century (83–87%). The finer resolution enables better understanding of the climatic variability and accurate hydrologic simulations across the UIB.

Most previous studies have used coarse-resolution GCMs focusing on larger river basins. Although such studies have shown reliable runoff projections over larger basins, regional conditions are often neglected. The coarse resolution climate models may be insufficient to simulate the complex climatic processes like monsoon in high mountainous regions, where higher resolution RCMs are essential (Sanjay *et al.* 2017). The climate simulated with RCMs in the Himalayas has shown well-represented physical processes like moisture transport (Dimri *et al.* 2013). The Atmospheric General Circulation Model (AGCM) provides climate projections at fine resolutions and shows the influence of monsoon and winter precipitation across the UIB.

Our study focuses on the entire UIB as well as three representative sub-basins to reveal their responses to climate change. The three selected sub-basins have different topography and climate characteristics, which are ideal for understanding inter-basin hydro-climatic variability. This study employs the Meteorological Research Institute-Atmospheric General Circulation Model (MRI-AGCM) with a spatial resolution of 0.1875°. The model simulates four scenarios based on different spatial patterns in sea surface temperatures (Mizuta *et al.* 2012). The fine-spatial resolution has enabled us to simulate the distinct spatial patterns of precipitation across the UIB (Supplementary material, Figure S1). The objectives of this study are as follows:

- Simulate the hydrological cycle of the UIB and its sub-basins with a distributed hydrological model forced by climate datasets. Snow and glacier melt models are coupled with the hydrological model based on geographic datasets including land use and glacier cover datasets. By conducting various scenario simulations, we quantify the runoff components of river flows from different sources including rainfall, snowmelt, and glacier melt.
- Assess the impacts of climate change on the stream flow of the UIB and its sub-basins. The runoff components are projected under future climate conditions to better understand the future stream flow changes in the entire UIB and its sub-basins.

The next section explains the study area including the topography and climate followed by the methodology with detailed descriptions of the models used in this study. The results and conclusions are presented in the last two parts.

2. STUDY AREA AND USED DATA

The UIB has an area of 192,861 km^2, and the mountainous region has an elevation range of ~6,800 m (Figure 2). The total glacier area in the basin is 14,087 km^2, and most of the mass is concentrated in the northwestern region (ICIMOD 2011). The UIB receives runoff from the Himalayas, Karakoram, and Hindukush mountains, which mostly consist of melt from snow and glaciers (Lutz *et al.* 2014). Supplementary material (Figures S2 and S3) shows the spatial distribution of glaciers in the basin. To assess the climatic and runoff conditions at the regional level, three representative sub-basins across the UIB, namely, Gilgit, Shigar, and Kharmong were selected. These sub-basins cover the entire geographic range and differ in terms of glacier coverage and climate (Figure 2). The Gilgit sub-basin is located at the western edge of the UIB and has an elevation of 1,472–6,392 m. Glacier coverage in the basin is 1,684 km^2 (13.2%) with almost 1,181 km^2 (70%) of the glaciers located in the elevation band of 4,000–5,000 m. The Kharmong sub-basin is located in the eastern region of the UIB, it is 70,000 km^2 and 3.6% of which is glacier covered. The Shigar sub-basin lies in the northern region and has an area of 6,900 km^2. It has the largest glacier coverage (28.8%) among the sub-basins (Table 1).

The observed monthly discharge (1980–2005) at the Bisham Qila is shown in Supplementary material, Figure S4. The hydrograph shows a peak in summer (May–September) which is due to the contribution of the meltwater (Mukhopadhyay & Khan 2014). In winter (October–April), the average monthly flow is sustained at approximately 450 m^3/s. This base flow is mainly due to the remnant melt and rainfall runoff, as explained by Mukhopadhyay & Khan (2015). For the sub-basin analysis, the river flow data of three sub-basins have also been acquired (Figure 2).

Downloaded from http://iwaponline.com/jwcc/article-pdf/13/9/3416/1114580/jwc0133416.pdf
by KYOTO UNIVERSITY user

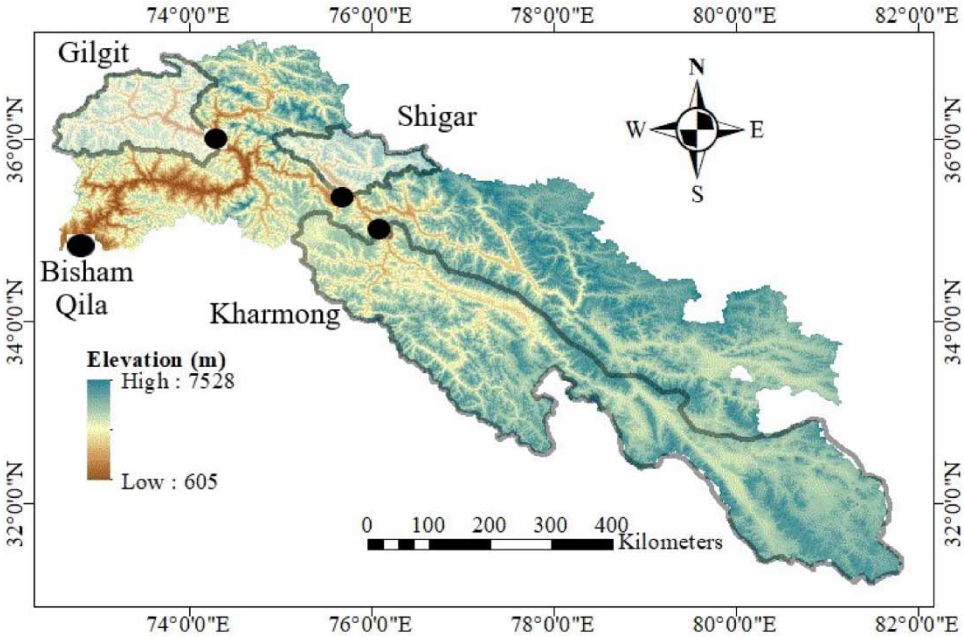

Figure 2 | The UIB and its sub-basins with their elevations and outlets.

Table 1 | Area, elevation, and glaciers of the UIB and sub-basins

Basin	Area (km^2)	Elevation (min, mean, and max) (m)	Glacier (%)
UIB	192,861	733, 4,600, 7,528	7.67
Gilgit	13,100	1,472, 4,030, 6,392	13.2
Shigar	6,900	2,189, 4,520, 7,360	28.8
Kharmong	70,000	2,409, 4,790, 6,470	3.6

For hydrological modeling of river flows, the 0.25° Asian Precipitation Highly Resolved Observational Data Integration Towards Evaluation (APHRODITE) (Yatagai *et al.* 2012) climate dataset was used along with glacier cover (ICIMOD 2011). Figure 3 and Supplementary material (Figure S5) show the average precipitation and temperature in the basin. The original APHRODITE dataset of precipitation was corrected using the precipitation extrapolation technique proposed by Immerzeel *et al.* (2015). They used glacier mass balance to estimate the precipitation gradient in the basin. Furthermore, these gradients are used to correct the precipitation bias in the APHRODITE dataset. The difference between our study and Immerzeel *et al.* (2015) is that they have done spatial downscaling of the APHRODITE dataset and performed bias-correction on the sub-basin level within the UIB. According to the dataset, winter (November–April) receives more precipitation than summer (May–October). Higher elevation zones receive heavy precipitation in winter in the form of snowfall. The eastern edge of the UIB is shown to have a high rate of precipitation in summer because of the monsoon influence (Figure 3). The snow cover for the calibration of the model is extracted from the MODIS product (MOD10A2) with a 500-m resolution (Hall & Riggs 2001).

3. METHOD

The rainfall–runoff–inundation (RRI) model introduced below was run with snow and glacier melt models. The rainfall, snowmelt, and glacier melt were calculated for each grid cell of the APHRODITE climate data using daily time series. For snow and glacier melt, separate degree-day models were used which require daily precipitation, daily temperature, and topographic information (Figure 4).

Downloaded from http://iwaponline.com/jwcc/article-pdf/13/9/3416/1114580/jwc0133416.pdf
by KYOTO UNIVERSITY user

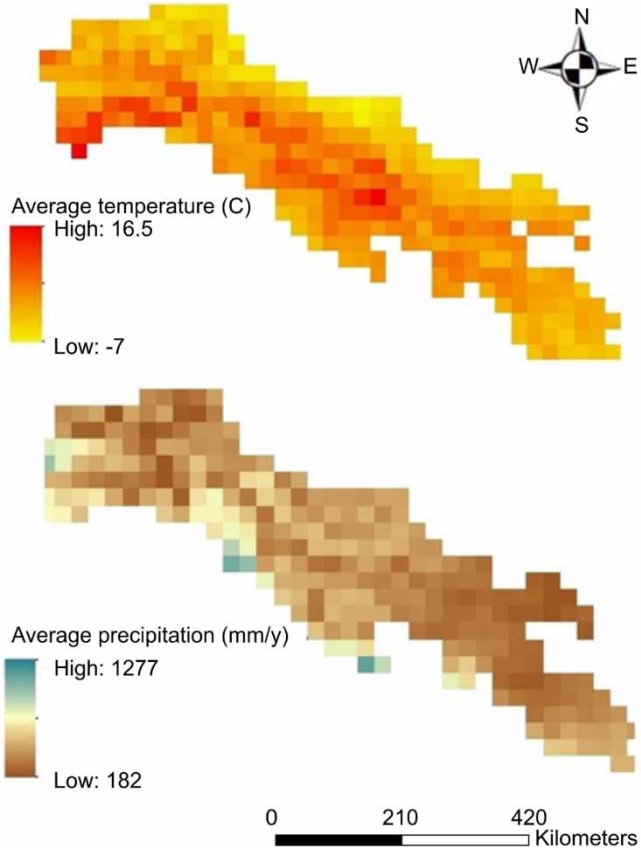

Figure 3 | Spatial distribution of average temperature and precipitation in the UIB (1980–2005).

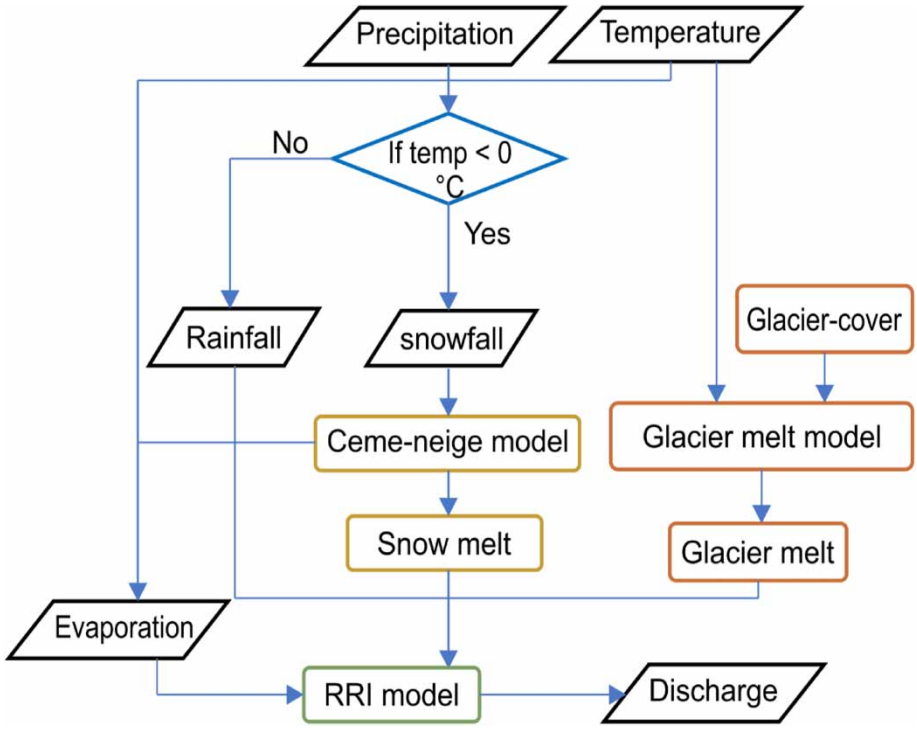

Figure 4 | Flow chart explaining the data and models used in this study.

Downloaded from http://iwaponline.com/jwcc/article-pdf/13/9/3416/1114580/jwc0133416.pdf
by KYOTO UNIVERSITY user

The simulation period consisted of 26 years from 1980 to 2005. The simulation was divided into two periods, one for calibration and the other for validation. The calibration covered 13 years from 1980 to 1992, whereas the validation covered the remaining years. The model was calibrated and validated with observed river flows at Bisham Qila, and the performance was checked using several statistical parameters. The river flows at sub-basins were validated with the observed river flows and simulated snow covers were compared with the MODIS snow cover.

3.1. Cema-Neige snow melt model

The Cema-Neige snow melt model was adopted from Valéry *et al.* (2014). This is a degree-day melt model that uses mean air temperature (T_{mean}) to distinguish between rainfall and snowfall. The main outputs of the model are rainfall and snowmelt for each grid cell of the APHRODITE data. In this application, if the temperature is below 0 °C, all precipitation is considered to be snow, otherwise it is treated as rainfall when the temperature is above 0 °C.

The snowpack temperature ($\text{Snowpack}_{\text{temp}}$) defines the internal thermal state of the snowpack, which is used to quantify the melt. If the internal temperature rises to 0 °C, the melt takes place. Equation (1) estimates the snowpack temperature.

$$\text{Snowpack}_{\text{temp},t} = \min\begin{cases} 0 \\ X*\text{Snowpack}_{\text{temp},t-1} + (1-X)* T_{\text{mean}} \end{cases} \quad (1)$$

where $\text{Snowpack}_{\text{temp},t}$ is the snowpack temperature at time step t in °C and X is the snowpack inertia factor, which is set by calibration. The potential melt Melt_{pot} (mm/day) is computed when the snowpack temperature reaches 0 °C and the daily mean air temperature is greater than 0 °C.

$$\text{Melt}_{\text{pot}} = \text{DDF}_s* T_{\text{mean}} \quad (2)$$

where DDF_s ($\text{mm°C}^{-1}\ \text{day}^{-1}$) is the degree-day factor. The melt cannot exceed snow storage, i.e. Melt_{pot} is limited to the snow storage. The accumulation of snow is updated daily based on the previously stored snow and the sum of solid precipitation as P_{snow} as indicated by the following equation.

$$\text{SS}_t = \text{SS}_{t-1} + P_{\text{snow}} - \text{Melt}_{\text{act}} \quad (3)$$

where SS_t (mm) is the snow storage at time step t updated after the accumulation or melt of snow (mm), and Melt_{act} is the actual melt (mm/day). Then actual melt Melt_{act} (mm/day) is estimated by the following empirical expression (Equation (4)). The snow cover area is also employed in this function as follows:

$$\text{Melt}_{\text{act}} = (0.9*\text{snow cover area} + 0.1)* \text{Melt}_{\text{pot}} \quad (4)$$

The snow cover area is a unique feature of the model. The model uses P_{snow} and annual average snowfall to estimate the percentage of the river basin covered with snow (Equation (5)).

$$\text{Snow cover area} = \begin{cases} \text{SS}_t/\text{TPS} & \text{if} \quad \text{SS}_t < 0.9*Z \\ 1 \end{cases} \quad (5)$$

where Z is the average annual snow precipitation (mm). More detailed information on Cema-Neige can be found in Valéry *et al.* (2014).

3.2. Glacier melt model

For the present climate glacier melt calculation, we used the glacier coverage estimated by ICIMOD (2011). For each grid of the APHRODITE, the glacier cover (%) is calculated and the glacier melt was quantified using a degree-day model explained by Terink *et al.* (2015). Equation (6) was used to calculate the daily melt from clean ice and debris-covered glaciers.

$$\text{Melt}_{\text{CI/DC}} = \begin{cases} \text{DDF}_{\text{CI/DC}}*T_{\text{mean}}* F_{\text{CI/DC}} & \text{if} \quad T_{\text{mean}} > 0 \\ 0 & \text{if} \quad T_{\text{avg}} \leq 0 \end{cases} \quad (6)$$

Downloaded from http://iwaponline.com/jwcc/article-pdf/13/9/3416/1114580/jwc0133416.pdf
by KYOTO UNIVERSITY user

where $\text{Melt}_{CI/DC}$ refers to the daily glacier melt from clean ice and debris-covered glacier, $\text{DDF}_{CI/DC}$ ($\text{mm°C}^{-1}\ \text{day}^{-1}$) are the degree-day factors and $F_{CI/DC}$ are the proportion of clean ice and debris-covered glaciers in the grid. The degree-day factors are set by the model calibration. The total glacier melt is the sum of both Melt_{CI} and Melt_{DC}.

3.3. Glacier area

In this study, the future glacier area was extracted from the estimates given by Huss & Hock (2015). Their study simulated the average glacier area in the future using 14 GCMs for the western parts of South Asia, where the UIB is located. The projected average glacier area for the entire western South Asia by 2075–2099 is 9,144 km^2. This is roughly 28% of the present area, which is 32,814 km^2 (Supplementary material, Figure S6). In this study, we assume the same ratio of glacier loss in the UIB region as estimated by Huss & Hock (2015) for the entire region of western South Asia. Thus, we assume that the current glacier area of 14,068 km^2 in the UIB will reduce to 3,521 km^2 by 2075–2099. In terms of the spatial variation of the glacier cover under future climate conditions, we also theorize that the glacier area will mainly be lost from the lowest elevation areas due to the higher temperatures; this pattern of glacier evolution is confirmed by Huss *et al.* (2010).

It should be noted that there are several glacier mass balance models, e.g. volume–area scaling, finite-element ice-flow models, etc. In addition to this, Huss *et al.* (2010) introduced empirical formulae to quantify the change in the thickness of glaciers. Their formulae are the result of field studies and topography analysis of 34 glaciers of varying sizes. Furthermore, they compared the results with a three-dimensional (3D) ice-flow model and found the empirical model performs satisfactorily. Compared to those physically based glacier models, our approach here based on temperature-based melt models is fairly simple. However, the advantage of the approach in this study can be based on the robust glacier area projected by the previous study, in this case by Huss & Hock (2015), and the use of the consistent degree-day factors for both glacier and snow melt, which enables us to interpret the results more directly.

3.4. GCM downscaling

The delta-change method was selected to remove the biases in temperature present in the MRI-AGCM. This method is a widely used technique that considers the mean bias as the difference between the observed and GCM data (Miao *et al.* 2016). The future projection can be adjusted as (Equation (7)):

$$\tilde{x}_{m-p.\text{adjust}} = x_{m-p} + (\bar{x}_{o-c} - \bar{x}_{m-c}) \tag{7}$$

where x is the meteorological variable of either o (observed) or m (modeled) for a historic training period or current climate (c) or future projection (p). Linear correction is another bias-correction technique that utilizes a scaling factor between observed and GCM simulations to reduce the bias in future projection. This is used for the bias correction of precipitation data as suggested by many previous studies, for example Miao *et al.* (2016) (Equation (8)).

$$\tilde{x}_{m-p.\text{adjust}} = x_{m-p} \cdot \left(\frac{\bar{x}_{o-c}}{\bar{x}_{m-c}}\right) \tag{8}$$

Future climate scenarios in the UIB and sub-basins are explained with the help of figures in the results section.

3.5. RRI model

The outputs of the Cema-Neige model (rainfall and snow melt) and glacier melt model were used for the simulation of the river flows using the RRI model. The original RRI model uses only rainfall and potential evapotranspiration as the input together with DEM and land use. In this study, we used the Cema-Neige model to first distinguish precipitation between rainfall and snowfall and update the snow coverage and snow melt as well as evapotranspiration. In the case of no-snow coverage with rainfall, we give the rainfall and glacier melt as the input of the RRI model. In the case of snow coverage existence, we give either rainfall or snowmelt depending on the form of precipitation along with the glacier melt as the input of the RRI model. The RRI model is a two-dimensional (2D) model that is capable of simultaneously representing rainfall runoff and flood inundation (Sayama *et al.* 2012). The flow on the slope grid cells was calculated using the 2D diffusive wave model, while the channel flow was calculated using the 1D diffusive wave model.

For better representations of RRI processes, the model simulates lateral subsurface flow, vertical infiltration flow, and surface flow. The vertical infiltration flow was estimated using the Green–Ampt model (Sayama 2015).

Downloaded from http://iwaponline.com/jwcc/article-pdf/13/9/3416/1114580/jwc0133416.pdf
by KYOTO UNIVERSITY user

4. RESULTS AND DISCUSSIONS

4.1. Model calibrations and validations

The simulated discharge at the Bisham Qila and sub-basins are shown in Figure 5, Supplementary material (Figures S7, S8, and S9), and the model performance is summarized in Table 2. Both the simulated and observed hydrographs show good agreement. For checking the performance of the simulations Nash–Sutcliffe (NS) coefficient, root-mean-square error (RMSE), and percent bias (PBIAS) have been calculated. The NS of 0.54–0.6 at the Bisham Qila is higher than the sub-basins indicating room for improvement in the simulation process.

A comparison of snow-covered areas between the Cema-Neige simulations and MODIS imagery is shown in Figure 6, which shows snow cover from 2000 to 2004.

The Cema-Neige model does not consider the slope and aspect of the grid cell in the simulation, which is not the exact representation of the physical process. In addition, an important parameter of the Cema-Neige model is the division of precipitation into rainfall and snowfall, which is based on using a 0 °C threshold. These factors are the sources of disagreement between the model results and the actual snow cover. Overall, simulations show satisfactory results, but improvements are required in the calibration of summer flows.

4.2. Estimation of snow and glacier contributions under present climate

Figure 7 shows the monthly contribution of rainfall, snowmelt, and glacier melt to the discharge. Under the current climate conditions, glaciers contribute 68%, rainfall 20%, and snowfall 12% of river flows. Rainfall runoff is generated mainly from May to October, and the maximum rainfall discharge occurs in September. With the increasing temperature in April, snow starts to melt from the lower elevation zones, and its discharge reaches approximately 1,000 m^3/s in April and approximately 2,400 m^3/s in May. The river flows continue to increase in the following months because of the inclusion of glacier melt. In summer from June to September, glacier melt dominates the hydrograph and contributes 85% of the total flow.

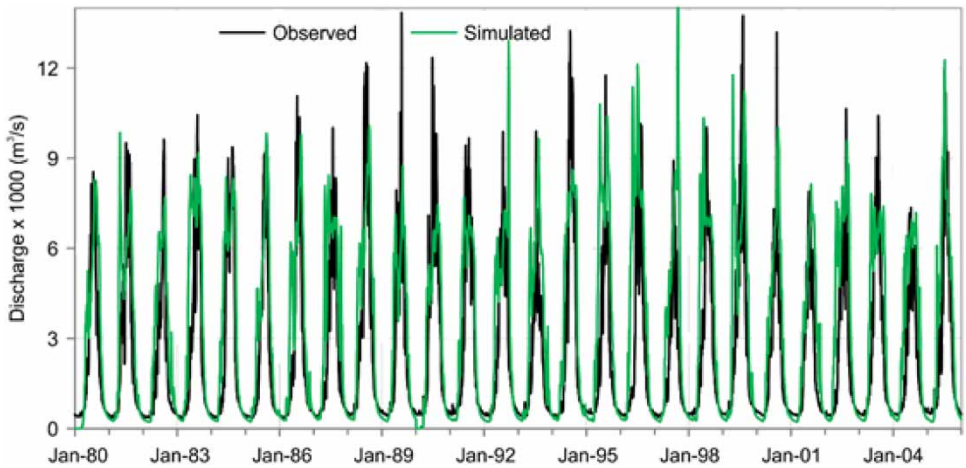

Figure 5 | Calibration and validation results of the hydrological model at Bisham Qila.

Table 2 | Nash–Sutcliffe (NS) coefficient, PBIAS, and root-mean-square error (RMSE) between the simulations and observed river flows in the UIB and sub-basins

	Calibration			Validation		
Station	**NS**	**PBIAS**	**RMSE (m^3/s)**	**NS**	**PBIAS**	**RMSE (m^3/s)**
Bisham	0.60	0.35	0.58	0.54	0.32	0.61
Gilgit	0.53	0.035	0.75	0.57	0.04	0.7
Shigar	0.50	0.3	0.7	0.48	0.27	0.68
Kharmong	0.45	0.28	0.72	0.41	0.32	0.64

Downloaded from http://iwaponline.com/jwcc/article-pdf/13/9/3416/1114580/jwc0133416.pdf
by KYOTO UNIVERSITY user

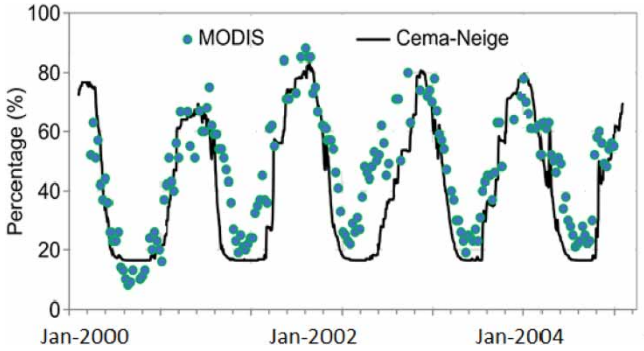

Figure 6 | Comparison of MODIS snow cover with simulated snow cover.

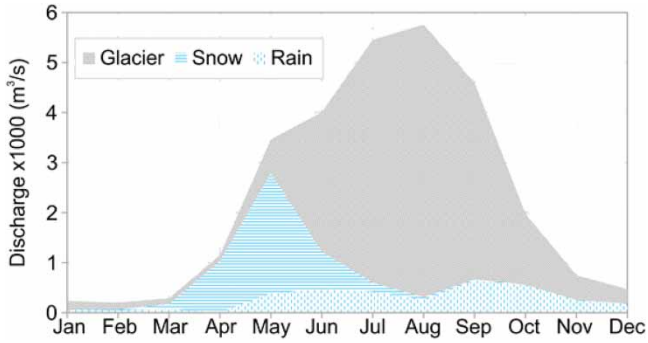

Figure 7 | The monthly contribution of glacier, snow, and rain in the UIB (1980–2005).

Lutz *et al.* (2014) reported the annual glacier contribution in the UIB at the Bisham Qila to be 67%, which is similar to that of our simulations (Table 3). Upon the comparison of runoff components with other studies, differences among estimates were found because of different scales of the study area, estimation approaches, datasets, etc.

4.3. Sub-basin river simulations

In total, runoff from these three sub-basins contributes to 40% of river flow at the Bisham Qila station, and in the glacier contribution, the sub-basins' share is 34%. Figures S7, S8, and S9 show simulations of discharge for Gilgit, Shigar, and Kharmong, respectively. They are highly glacierized, and the runoff is meltwater-dependent. The common characteristics of runoff in the three sub-basins in the UIB are the significant proportion of melt-runoff, which explains the significance of winter precipitation in the basin (Table 3).

In Gilgit and Shigar, over three-fourths of the annual river flows are contributed by meltwater alone because of heavy winter precipitation and larger glacier covers. In Kharmong, rainfall runoff is higher than snow and glacier melt because of the stronger influence of monsoon precipitation (Table 3).

4.4. Future climate in the UIB

Figure 8 shows the change in basin temperature and precipitation during 2075–2099 based on the four MRI-AGCM scenarios with different SST patterns. Across the UIB, the temperature will increase by 5.3 °C, and the largest increase of 6.6 °C is projected in June, July, and August (JJA). In December, January, and February (DJF), the temperature will increase by 4.5 °C. The comparison with other studies in Table 4 suggests that the increase in annual temperature is similar to the other studies based on different GCMs or RCMs. Note that the annual temperature rise reported by Su *et al.* (2016) is relatively smaller (+3.8 °C) but this is mainly due to their target period that is between 2041 and 2070.

In terms of annual precipitation change, our study projects its increase by 17%. In particular, the precipitation in the JJA season shows a higher increase by 35%, indicating a wet summer season. Furthermore, the winter precipitation is also projected to increase which could increase the snow depth and spring runoff. The projections of annual precipitation

Downloaded from http://iwaponline.com/jwcc/article-pdf/13/9/3416/1114580/jwc0133416.pdf
by KYOTO UNIVERSITY user

Table 3 | Summary of precipitation (*P*) (mm), temperature (*T*) (°C), runoff (*Q*), and glacier coverage (%) in (a) the present (1980–2005) and (b) the future (2075–2099)

Stations	*P* (mm)	*T* (°C)	*Q* (mm)	Glacier (Q_g)	Snow (Q_s)	Rain (Q_r)	Glacier (%)
(a) Present (1980–2005)							
Bisham	440	1.77	656	367 (68)	62 (12)	105 (20)	7.67
Gilgit	491	1.34	962	614 (75)	77 (10)	123 (15)	13.2
Shigar	450	−1.67	2,400	1,805 (85)	145 (7)	151 (8)	28.8
Kharmong	405	2.18	226	57 (35)	42 (26)	63 (39)	3.6
(b) Future (2075–2099)							
Bisham	516	7.4	566	280 (60)	33 (7)	150 (33)	1.83
Gilgit	553	7.9	272	36 (17)	41 (19)	136 (64)	2
Shigar	642	6.7	1,640	1,128 (81)	87 (6)	176 (13)	12.5
Kharmong	453	6.6	357	137 (50)	20 (7)	116 (43)	3.5

Note: Runoff contributions by glacier (Q_g), snow (Q_s), and rain (Q_r) are expressed in mm. Values in the parenthesis show the percentage of the given components in the runoff.

summarized in Table 4 show higher variations among different GCMs and RCMs by different studies. For example, four selected GCMs by Lutz *et al.* (2016) indicated the range between −25 and 125% depending on the GCMs.

The spatial pattern in future temperature change is fairly homogeneous across sub-basins (Figure 9). The difference among the SST scenarios was also not very evident. On the other hand, the precipitation changes according to the MRI-AGCM are spatially more variable. In winter (October–March), precipitation will increase in most of the basins with some differences in the magnitudes. For the season between April and September, the eastern region of the UIB is projected to increase even up to 100% and the western part of the UIB showed some decreasing trend in the seasonal precipitation (Figure 10). Among the

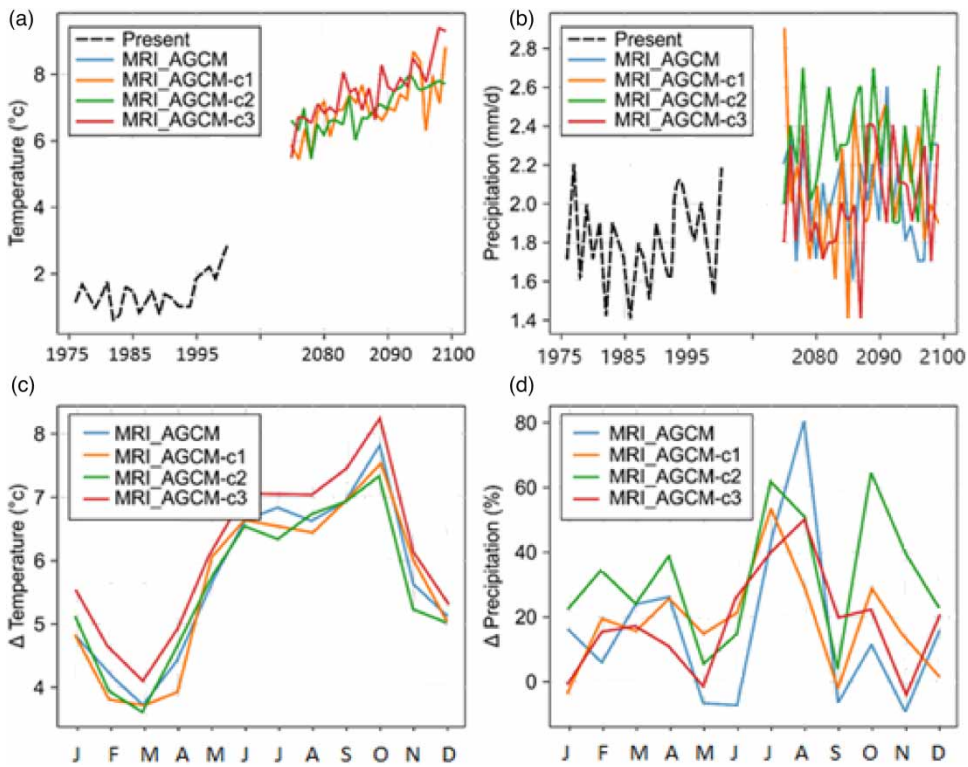

Figure 8 | Change in (a) temperature and (b) precipitation across the Upper Indus River Basin according to MRI-AGCM. Change in (c) temperature and (d) precipitation on a monthly basis in the future (2075–2099).

Downloaded from http://iwaponline.com/jwcc/article-pdf/13/9/3416/1114580/jwc0133416.pdf
by KYOTO UNIVERSITY user

Table 4 | A comparison of climate change impact studies in the UIB with this study

	This study	(a) Lutz *et al.* (2016))	(b) Su *et al.* (2016)	(c) Hasson *et al.* (2019)	(d) Ali *et al.* (2015)	(e) (Babur *et al.* 2016)	(f) Khan *et al.* (2020)
Future period to be studied	2075–2099	2071–2100	2041–2070	2070–2099	2071–2100	2071–2100	2071–2100
The definition of UIB	Upstream of Bisham Qila	Upstream of Bisham Qila and other sub-basins including the Kabul, Jhelem, Chenab, Satluj. At Bisham Qila for the discharge	The region in UIB which is above 2,000 m	Upstream of Bisham Qila and the Kabul river basin	Upstream of Bisham Qila	Mangla River Basin in the south of UIB	Upstream of Bisham Qila
Used GCMs and scenarios	MRI-AGCM, RCP8.5, four SSP patterns	Four selected GCMs (MPI-ESM-LR, IPSL-CM5A-LR, CSIRO-Mk3-6 – 0, MIROC5), RCP8.5 (in this table)	20 GCMs from CMIP5, RCP8.5 (in this table)	RegCM4.3, RCP8.5 (in this table)	Two GCMs (CCAM and RegCM), RCP8.5 (in this table)	7 GCMs (RCP4.5 and 8.5)	5 CORDEX RCMs
Glacier meltmodels	Future glacier cover is estimated based on Huss & Hock (2015) and temperature-index for the melting	Glacier mass-balance model included based upon temperature-index	Glacier mass-balance model included based upon temperature-index	No direct glacier meltmodel but a temperature-index snow meltmodel	No direct glacier melt model but an energy-based snow meltmodel	SWAT model which has no direct glacier model	SWAT model which has no direct glacier model
Method to estimate the glacier coverage for present climate	ICIMOD database	Randolph glacier Inventory	Randolph glacier Inventory	–	–	–	–
Projected annual temperature change (°C)	+5.3(+5.14 ~ + 5.64)	+6.5(+5.5 ~ +8.0)	+3.8	+5.1	+5.8	+5.4	+6.2
Projected annual precipitation change (%)	+17.0(10–21)	+10.6 (−25 to +125)	+4.5	30 to +40	+20.7	+26	+38
Projected annual discharge change (%)	−14(−16 to −10)	30(−15 to +60)	6–22	17.4	87	−27 to +74	+8(−27 to +27)
Monthly temperature change (°C)							
DJF	4.6	6.3	3.9	3.6	6.5	5.58	-
MAM	4.6	6.0	3.7	3.7	6.1	6	

(*Continued.*)

Downloaded from http://iwaponline.com/jwcc/article-pdf/13/9/3416/1114580/jwc0133416.pdf
by KYOTO UNIVERSITY user

Table 4 | Continued

	This study	(a) Lutz *et al.* (2016))	(b) Su *et al.* (2016)	(c) Hasson *et al.* (2019)	(d) Ali *et al.* (2015)	(e) (Babur *et al.* 2016)	(f) Khan *et al.* (2020)
JJA	6.6	6.15	3.6	5.4	5.9	4.72	
SON	5.3	5.8	3.7	3.9	5.05	5.28	
Monthly precipitation change (%)							
DJF	12	16	1	−20	3.5	0.58	
MAM	14	−18	−2	18	32.9	20	
JJA	35	15	13	33	13	53	
SON	−1.7	40	2.5	25	33.2	58	
Monthly discharge change (%)							
DJF	35	100	20	15	147	104	50
MAM	−12	110	47	264	300	20	200
JJA	−21	22	2	3	57	14	−46
SON	−5	60	29	0	124	52	43

SON, September, October, and November.

sub-basins we selected, the Kharmong sub-basin located in the eastern part of the UIB may experience a higher increase in the precipitation from July to September (Figure 10). On the contrary, the Shigar sub-basin located in the northern part of the UIB may show a decrease in precipitation in some seasons.

The trends in the change in the spatial features of the future precipitation can be confirmed by Figure 11 which shows the projected monthly changes in temperature and precipitation in the UIB and its three sub-basins. There is a consensus among the scenarios in terms of temperature change in the three sub-basins. An insightful variability exists in the precipitation

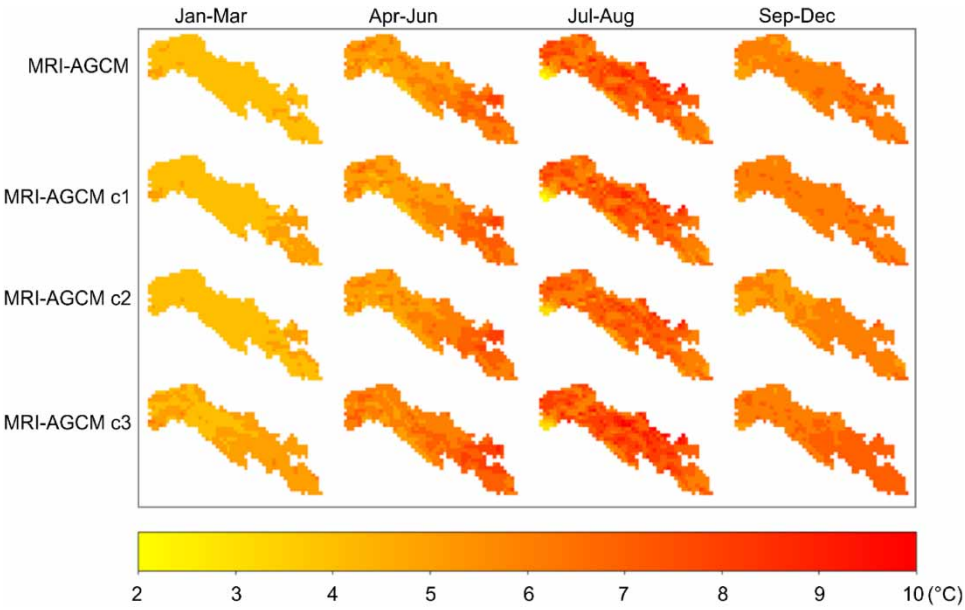

Figure 9 | Increase in temperature across four MRI-AGCM scenarios in the future based on seasons in the UIB.

Downloaded from http://iwaponline.com/jwcc/article-pdf/13/9/3416/1114580/jwc0133416.pdf
by KYOTO UNIVERSITY user

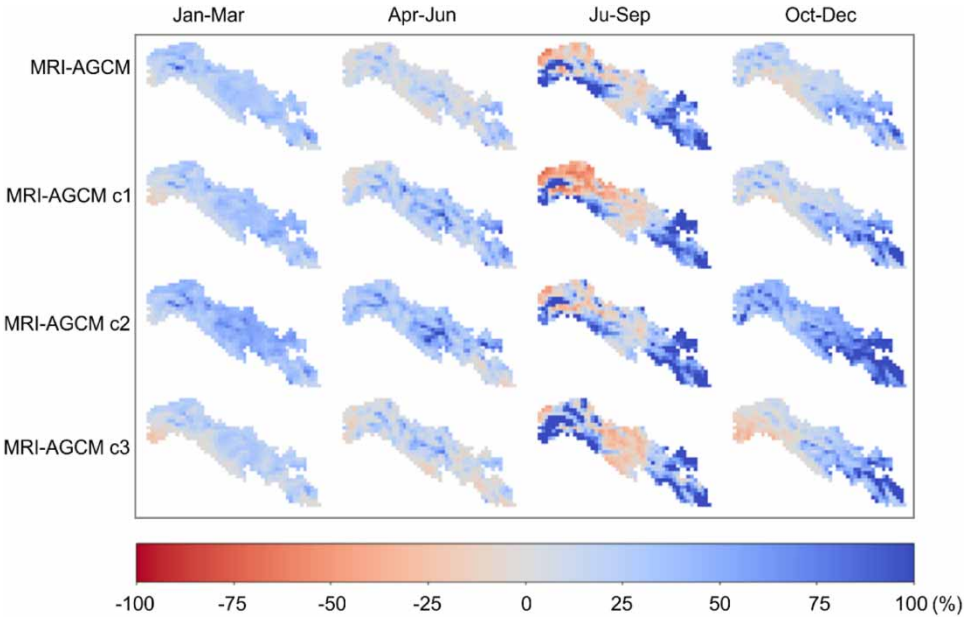

Figure 10 | Change in precipitation across four MRI-AGCM scenarios in the future based on seasons in the UIB.

regime; Shigar will have an increase in precipitation during October–April in the future, and in Gilgit during July–September, but a decrease in the other months. On the other hand, Kharmong lies adjacent to the Himalayan mountain range and it has a different precipitation regime, which is summer-dominated as opposed to that of Shigar and Gilgit. The precipitation during July–August is projected to increase by 60–80% in the sub-basin.

4.5. Future flow regime

Figure 12 shows the future (2075–2099) and present (1980–2005) monthly discharge at the Bisham Qila and its sub-basins. At the Bisham Qila and its sub-basins, significant shifts in the spring and summer hydrographs are evident. As summarized in Tables 3 and 4, at the Bisham Qila, annual river flows will decrease by 14% while the the monthly discharge will decrease by 12% in March–May (MAM) and 21% in JJA and increase by 35% in DJF. The patterns and magnitudes are different in the sub-basins because of the glaciers' elevations and prevalent climate regimes. The Gilgit and Shigar will be the most affected and face reduction of up to 70 and 32% in average annual flows (Table 3). In Gilgit, the decrease in pre-monsoon precipitation will negatively impact the river flows as well (Figure 11). The monthly discharge at Gilgit will decrease by 85% in JAS. The runoff in both of these basins will be impacted by the retreat of glaciers and higher evaporation because of warmer temperatures. Kharmong will have higher river flows (+58%) in the future because of the combined action of precipitation and excess glacier melt (Table 3).

Other studies have also projected changes in future monthly discharge in the UIB. For example, Lutz *et al.* (2016) showed that under the representative concentrative pathway (RCP)8.5 scenario, the annual discharge at the Bisham Qila will increase by 30% with a more significant increase by 100 and 110% in DJF and MAM, respectively (Table 4), mainly because of precipitation and temperature increases. Notably, the projection by Lutz *et al.* (2016) presented that under the RCP4.5 scenario, the runoff will decrease by approximately 20% at the Bisham Qila because the rate of increase in temperature is not as significant as in the RCP8.5 case. In that scenario, the reduction of the glacier coverage plays a more dominant role and consequently, the annual discharge is projected to be decreased. In that regard, our projection at the Bisham Qila is similar to the case of RCP4.5 by Lutz *et al.* (2016) as both of them project the reduction of annual discharge.

Figure 13 explains the shift in the runoff components by different sources including rainfall, snow, and glacier melt. At the outlets of the Bisham Qila and the sub-basins, rainfall–runoff is projected to increase because of higher precipitation in the summer and change in the phase of precipitation in the winter from snow to rainfall because of higher temperatures.

This phase change will negatively impact the snowmelt contribution, resulting in a decrease of its runoff by half of the present quantities. The runoff from glacier melt will also decrease, but the magnitudes are different depending on the elevation

Downloaded from http://iwaponline.com/jwcc/article-pdf/13/9/3416/1114580/jwc0133416.pdf
by KYOTO UNIVERSITY user

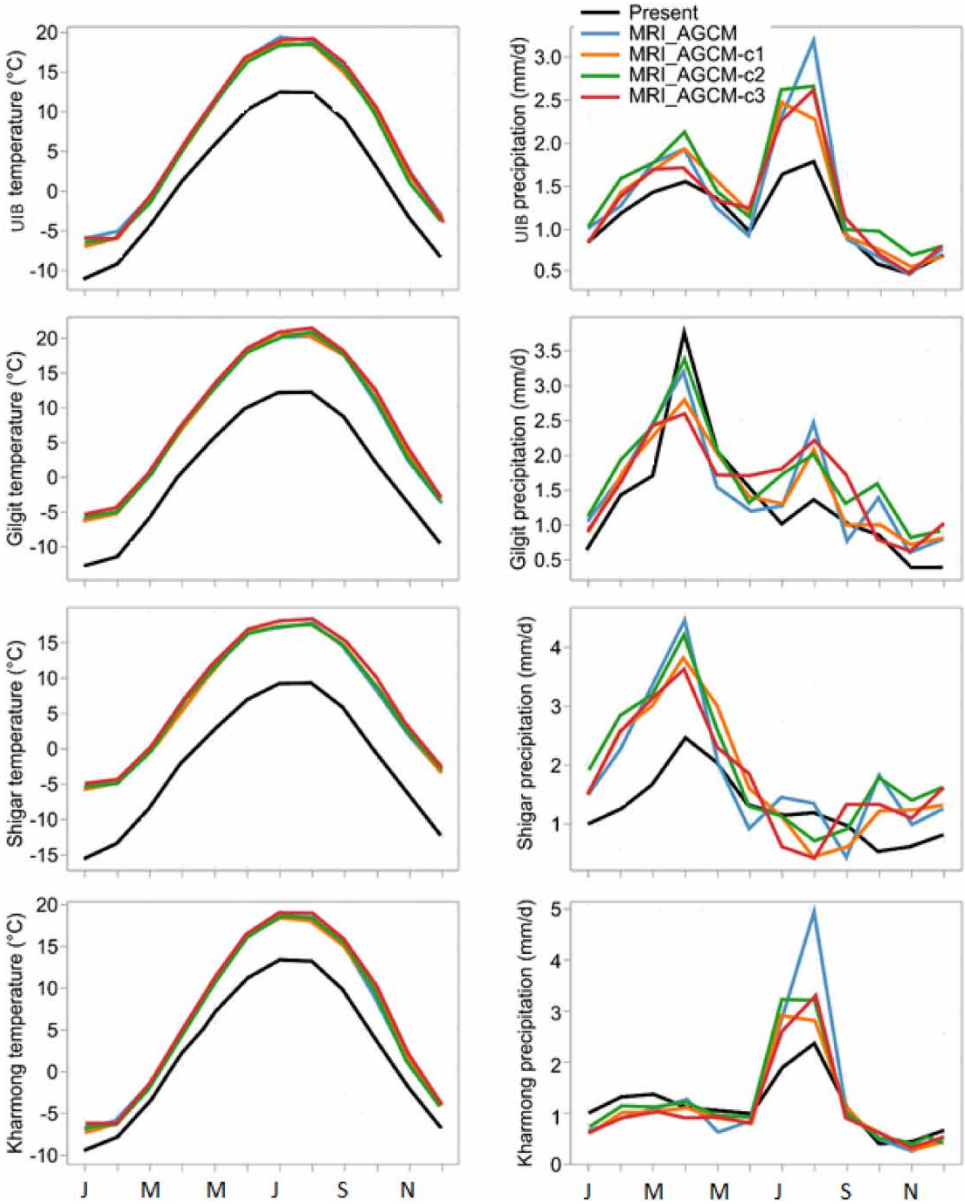

Figure 11 | Change in climate in the sub-basins of the UIB according to four MRI-AGCM scenarios (left: monthly temperature; right: monthly precipitation).

distribution of glaciers in the region. In Gilgit, the glaciers will retreat to the extent that it will diminish their contribution to the hydrograph because most of its glaciers are located below 5,000 m. Shigar will also experience a decrease in summer flows because of the glacier retreat and high evaporation. On the other hand, Kharmong will have an excess contribution of glaciers to the hydrograph because its glaciers are located at higher elevations compared to the other two sub-basins (Supplementary material, Figure S3) and (Table 3). Overall, the spring and summer season will be drier in the western region because of the deficit of meltwater in summer (Figure 14). On the other hand, the eastern region will see excess river flows because of wetter monsoon and largely intact glaciers which will melt with higher rates because of higher temperatures.

5. LIMITATIONS

The methodology of this research has a few shortcomings which have resulted in biases in the river flow simulations. The snow melt and glacier melt models depend upon the empirical degree-days approach which is reliable but approximates

Downloaded from http://iwaponline.com/jwcc/article-pdf/13/9/3416/1114580/jwc0133416.pdf
by KYOTO UNIVERSITY user

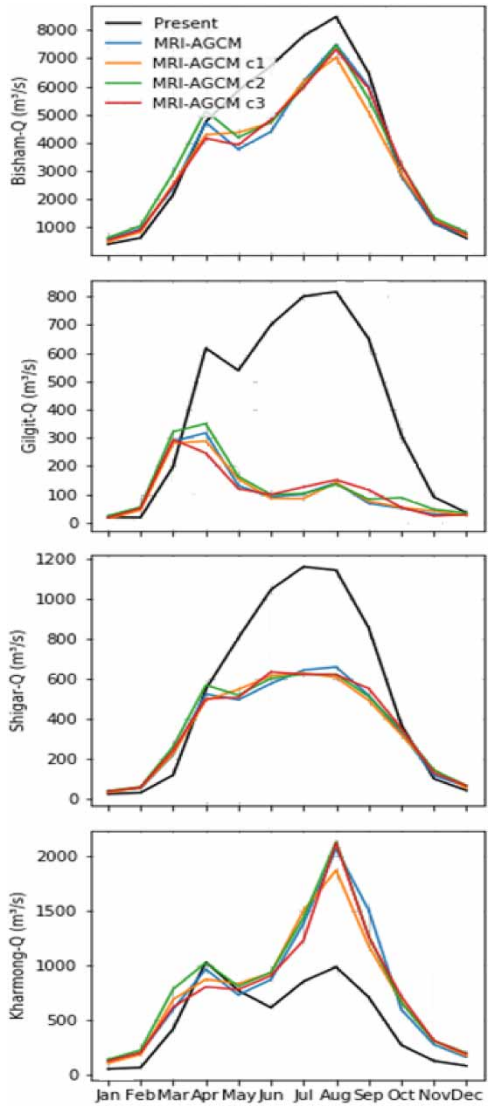

Figure 12 | Present (1980–2005) and future (2075–2099) river flows in the UIB and sub-basins. The first row shows Bisham, the second shows Gilgit, the third shows Shigar, and the last shows Kharmong. The present river flows are shown in black.

the physical processes. Another source of bias is the spatial resolution of the climate datasets and estimation of precipitation in the mountain regions (Immerzeel *et al.* 2015). For future projection of river flows, the extent of glaciers is estimated from Huss & Hock (2015) which could be improved by integrating a robust glacier mass-balance model to improve the accuracy of the simulations.

Atmosphere/Ocean General Circulation Models (AOGCMs) are the foundation for the simulation of the climatic response to anthropogenic activities and results from such simulations have provided the information for the majority of the climatic impact studies. However, the coarse resolution of AOGCMs raises constraints on their usefulness, especially in complex physiographic features. Therefore, high-resolution and time-slice AGCM experiments have been developed to improve the regional information of AOGCMs (Mearns *et al.* 2003). An AGCM is forced by observed SST and sea-ice distribution. Then, the future climate is simulated with the boundary conditions (SST and sea-ice), which are already projected by AOGCM (Mizuta *et al.* 2012). A high-resolution AGCM is vital for realistic precipitation simulations in mountainous regions and for obtaining meaningful future projections as well. A study used four-member 20-km MRI-AGCM and reported that the greatest extreme precipitation increases are found in the South Asian region (Kitoh *et al.* 2016).

Downloaded from http://iwaponline.com/jwcc/article-pdf/13/9/3416/1114580/jwc0133416.pdf
by KYOTO UNIVERSITY user

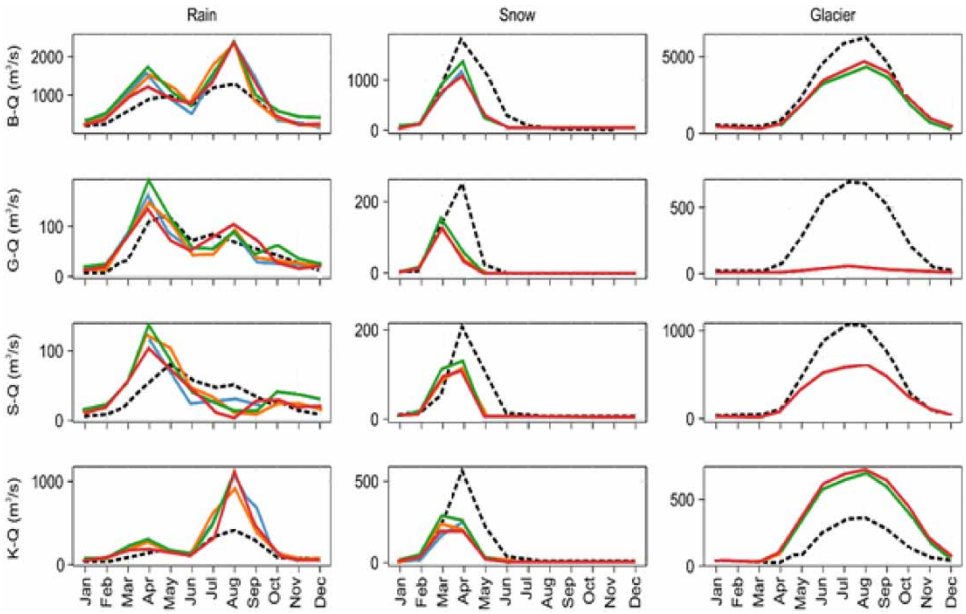

Figure 13 | Comparison between the present (1980–2005) and the future (2075–2099) runoff components of the UIB and sub-basins. Row wise, the simulations represent Bisham Qila, Gilgit, Shigar, and Kharmong, respectively. The black line represents the present and other colors MRI-AGCM.

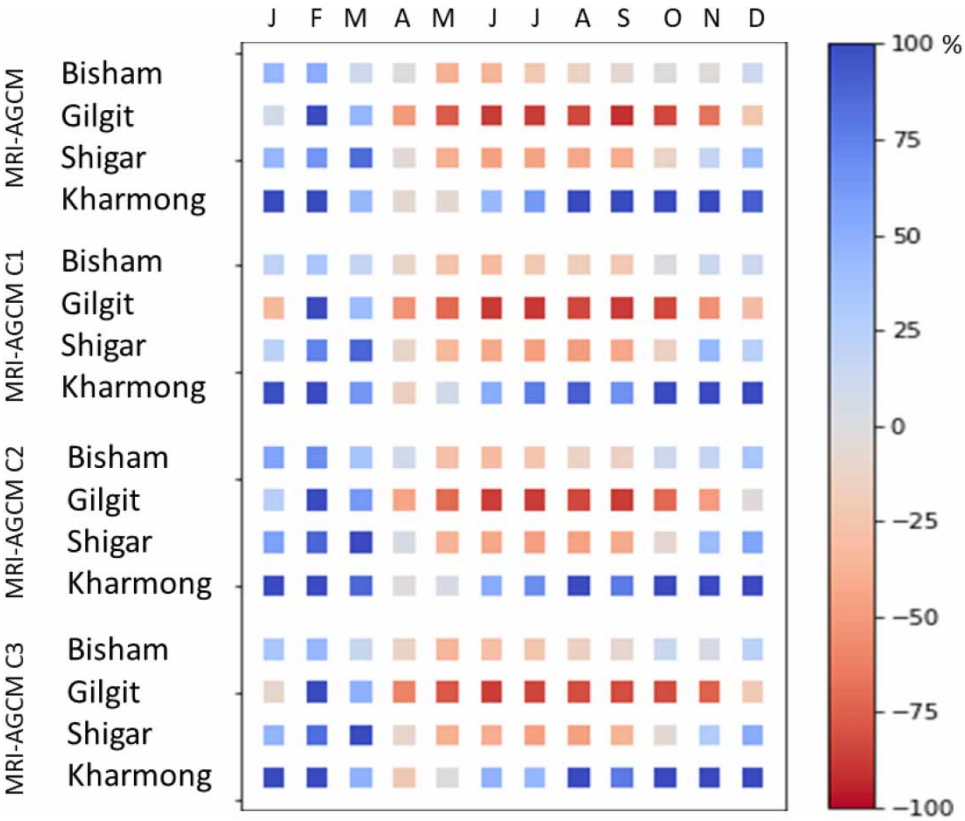

Figure 14 | Percentage changes in the monthly river flows in future (2075–2099) in the UIB and its sub-basins with respect to the present (1980–2005).

Downloaded from http://iwaponline.com/jwcc/article-pdf/13/9/3416/1114580/jwc0133416.pdf
by KYOTO UNIVERSITY user

Furthermore, Krishnan *et al.* (2015) used the high-resolution Laboratoire de Météorologie Dynamique general circulation model (LMDZ) and found a robust increase in the frequency of heavy precipitation (>100 mm/day) over central India.

The fine-resolution MRI-AGCM also contains some biases and uncertainties. For example, Rahman *et al.* (2013) and Rajendran *et al.* (2012) employed them in India and Bangladesh to study the monsoon precipitation and found biases in the monsoon precipitation because of the dependence of the simulations on a specific scenario of greenhouse gas emission and boundary conditions. Another study reported that the Asian monsoon precipitation is sensitive to the cumulus parameterization schemes rather than SST (Endo *et al.* 2012). Therefore, the inclusion of a coupled air-ocean model with AGCM while projecting present and future climate will yield more reliable projections.

The biases of the MRI-AGCM could affect the simulations of the summer river flows in the UIB, especially in the eastern region where monsoon is more prevalent. Nevertheless, MRI-AGCM is a step forward in the climate modeling because of its resolution and improved physical parameterizations which have improved the simulations of heavy monthly-mean precipitation around the tropical Western Pacific, the global distribution of tropical cyclones, and the seasonal march of East Asian summer monsoon (Kitoh *et al.* 2016).

6. CONCLUSIONS

The UIB is the major source of water for agricultural and domestic water demands in Pakistan. The UIB receives heavy winter precipitation and glaciers also contribute significant quantities of runoff annually. The river flows in the UIB are vulnerable to changing climate, which will cause an imbalance in the water supply and demand. Therefore, for the assessment of the impact of future climate on river flows, this study used the MRI-AGCM with the spatial resolution of 0.1875° and the RRI model coupled with snow and glacier melt models. The MRI-AGCM projected an annual increase of temperature by 5.3 °C and annual precipitation by 17% in the future (2075–2099). Although both temperature and annual precipitation are projected to increase, the annual river flow from the UIB was projected to decrease by 14% mainly due to the deficit in glacier runoff.

Furthermore, the timing of runoff will be altered by the climate change, i.e. increase by 35% in DJF while decrease by 12 and 21% in MAM and JJA, respectively. Our study demonstrated that such patterns are different across the UIB mainly because of the spatial variation in glacier melt and precipitation regime. Such regional analysis and information would be useful for better water management in the UIB and have been enabled because of the fine-spatial resolution of the AGCM.

The simulation can be improved by using finer and accurate climate datasets. Furthermore, the simulations require a robust glacier mass-balance model which will enhance the quality of the analysis. Hence, future studies should be done with dynamic modeling of glacier extent and coverage under future climate conditions.

ACKNOWLEDGEMENTS

Special thanks to the Water and Power Development Authority (WAPDA) and the Pakistan Meteorological Authority (PMD) for the provision of hydro-meteorological data.

FUNDING

S.B. was funded by the Japanese government through the MEXT scholarship for PhD studies at Kyoto University. In addition to this, the authors are thankful to Kyoto University for providing additional funding for data collection.

AUTHORS' CONTRIBUTIONS

S.B. and T.S. conceptualized the study. S.B. prepared the dataset and performed the modeling tasks. M.Y. contributed to the glacier melt analysis. S.B. wrote the manuscript and all the authors contributed to the review.

DATA AVAILABILITY STATEMENT

All relevant data are included in the paper or its Supplementary Information.

CONFLICT OF INTEREST

The authors declare there is no conflict.

Downloaded from http://iwaponline.com/jwcc/article-pdf/13/9/3416/1114580/jwc0133416.pdf
by KYOTO UNIVERSITY user

REFERENCES

Abbas, A., Ullah, S., Ullah, W., Waseem, M., Dou, X., Zhao, C., Karim, A., Zhu, J., Hagan, D. F. T., Bhatti, A. S. & Ali, G. 2022 Evaluation and projection of precipitation in Pakistan using the coupled model intercomparison project phase 6 model simulations. *Int. J. Climatol.* https://doi.org/10.1002/JOC.7602.

Ali, A. 2013 *Indus Basin floods: Mechanisms, Impacts, and Management*. Mandaluyong City.

Ali, S., Li, D., Congbin, F. & Khan, F. 2015 Twenty first century climatic and hydrological changes over Upper Indus Basin of Himalayan region of Pakistan. *Environmental Research Letters* **10**, 014007.

Ali, S., Reboita, M. S. & Kiani, R. S. 2021 21st century precipitation and monsoonal shift over Pakistan and Upper Indus Basin (UIB) using high-resolution projections. *Sci. Total Environ.* **797**, 149139. https://doi.org/10.1016/j.scitotenv.2021.149139.

Archer, D. 2003 Contrasting hydrological regimes in the upper Indus Basin. *Journal of Hydrology* **274**, 198–210.

Babur, M., Babel, M. S., Shrestha, S., Kawasaki, A. & Tripathi, N. K. 2016 Assessment of climate change impact on reservoir inflows using multi climate-models under RCPs – the case of Mangla Dam in Pakistan. *Water* **8**, 389. https://doi.org/10.3390/W8090389.

Dahri, Z. H., Moors, E., Ludwig, F., Ahmad, S., Khan, A., Ali, I. & Kabat, P. 2018 Adjustment of measurement errors to reconcile precipitation distribution in the high-altitude Indus basin. *Int. J. Climatol.* **38**, 3842–3860. https://doi.org/10.1002/joc.5539.

Dimri, A. P., Yasunari, T., Wiltshire, A., Kumar, P., Mathison, C., Ridley, J. & Jacob, D. 2013 Application of regional climate models to the Indian winter monsoon over the western Himalayas. *Sci. Total Environ.* **468–469**, S36–S47. https://doi.org/10.1016/J.SCITOTENV.2013.01.040.

Endo, H., Kitoh, A., Ose, T., Mizuta, R. & Kusunoki, S. 2012 Future changes and uncertainties in Asian precipitation simulated by multiphysics and multi-sea surface temperature ensemble experiments with high-resolution meteorological research institute atmospheric general circulation models (MRI-AGCMs). *J. Geophys. Res. Atmos.* **117**. https://doi.org/10.1029/2012JD017874.

Hall, D. K. & Riggs, G. A. 2001 *MODIS/Terra Snow Cover 8-Day L3 Global 500 m SIN Grid, Version 6 [WWW Document]*. Available from: https://nsidc.org/data/MOD10A2.

Hasson, S. U., Saeed, F., Böhner, J. & Schleussner, C. F. 2019 Water availability in Pakistan from Hindukush–Karakoram–Himalayan watersheds at 1.5 °C and 2 °C Paris agreement targets. *Adv. Water Resour.* https://doi.org/10.1016/j.advwatres.2019.06.010.

Huss, M. & Hock, R. 2015 A new model for global glacier change and sea-level rise. *Front. Earth Sci*. https://doi.org/10.3389/feart.2015.00054.

Huss, M., Jouvet, G., Farinotti, D. & Bauder, A. 2010 Future high-mountain hydrology: a new parameterization of glacier retreat. *Hydrol. Earth Syst. Sci.* **14**, 815–829. https://doi.org/10.5194/hess-14-815-2010.

ICIMOD 2011 *Clean Ice and Debris Covered Glaciers of HKH Region [WWW Document]*. Available from: http://apps.geoportal.icimod.org/hkhglacier.

Immerzeel, W. W., van Beek, L. P. H. & Bierkens, M. F. P. 2010 Climate change will affect the Asian water towers. *Science (80-.)* **328**, 1382–1385. https://doi.org/10.1126/science.1183188.

Immerzeel, W. W., Wanders, N., Lutz, A. F., Shea, J. M. & Bierkens, M. F. P. 2015 Reconciling high-altitude precipitation in the Upper Indus basin with glacier mass balances and runoff. *Hydrol. Earth Syst. Sci.* **19**, 4673–4687. https://doi.org/10.5194/hess-19-4673-2015.

Khan, A. J., Koch, M. & Tahir, A. A. 2020 Impacts of climate change on the water availability, seasonality and extremes in the Upper Indus Basin (UIB). *Sustainability*. https://doi.org/10.3390/su12041283.

Kiani, R. S., Ali, S., Ashfaq, M., Khan, F., Muhammad, S., Reboita, M. S. & Farooqi, A. 2021 Hydrological projections over the Upper Indus basin at 1.5 °C and 2.0 °C temperature increase. *Sci. Total Environ.* **788**, 147759. https://doi.org/10.1016/j.scitotenv.2021.147759.

Kitoh, A., Ose, T. & Takayabu, I. 2016 Dynamical downscaling for climate projection with high-resolution MRI AGCM-RCM. *J. Meteorol. Soc. Japan. Ser. II* **94A**, 1–16. https://doi.org/10.2151/jmsj.2015-022.

Krishnan, R., Sabin, T. P., Vellore, R., Mujumdar, M., Sanjay, J., Goswami, B. N., Hourdin, F., Dufresne, J. L. & Terray, P. 2015 Deciphering the desiccation trend of the South Asian monsoon hydroclimate in a warming world. *Clim. Dyn.* **47** (3), 1007–1027. https://doi.org/10.1007/S00382-015-2886-5.

Lutz, A. F., Immerzeel, W. W., Shrestha, A. B. & Bierkens, M. F. P. 2014 Consistent increase in High Asia's runoff due to increasing glacier melt and precipitation. *Nat. Clim. Change* **4**, 587–591. https://doi.org/10.1038/nclimate2237.

Lutz, A. F., Immerzeel, W. W., Kraaijenbrink, P. D. A., Shrestha, A. B. & Bierkens, M. F. P. 2016 Climate change impacts on the Upper Indus hydrology: sources, shifts and extremes. *PLoS One*. https://doi.org/10.1371/journal.pone.0165630.

Mcsweeney, C., New, M. & Lizcano, G. 2012 *UNDP Climate Change Country Profiles Pakistan*.

Mearns, L. O., Giorgi, F., Whetton, P., Pabon, D. & Lal, M. 2003 *Guidelines for Use of Climate Scenarios Developed from Regional Climate Model Experiments*.

Miao, C., Su, L., Sun, Q. & Duan, Q. 2016 A nonstationary bias-correction technique to remove bias in GCM simulations. *J. Geophys. Res. Atmos.* **121**, 5718–5735. https://doi.org/10.1002/2015JD024159.

Mizuta, R., Yoshimura, H., Murakami, H., Matsueda, M., Endo, H., Ose, T., Kamiguchi, K., Hosaka, M., Sugi, M., Yukimoto, S., Kusunoki, S. & Kitoh, A. 2012 Climate simulations using MRI-AGCM3.2 with 20-km grid. *J. Meteorolog. Soc. Japan* **90A**, 233–258. https://doi.org/10.2151/jmsj.2012-A12.

Downloaded from http://iwaponline.com/jwcc/article-pdf/13/9/3416/1114580/jwc0133416.pdf
by KYOTO UNIVERSITY user

Mukhopadhyay, B. & Khan, A. 2014 A quantitative assessment of the genetic sources of the hydrologic flow regimes in Upper Indus basin and its significance in a changing climate. *J. Hydrol.* **509**, 549–572. https://doi.org/10.1016/j.jhydrol.2013.11.059.

Mukhopadhyay, B. & Khan, A. 2015 A reevaluation of the snowmelt and glacial melt in river flows within Upper Indus Basin and its significance in a changing climate. *Journal of Hydrology* **527**, 119–132.

Ougahi, J. H., Cutler, M. E. J. & Cook, S. J. 2022 Modelling climate change impact on water resources of the Upper Indus Basin. *J. Water Clim. Change* **13**, 482–504. https://doi.org/10.2166/wcc.2021.233.

Rahman, M. M., Rafiuddin, M., Alam, M. M., Kusunoki, S., Kitoh, A. & Giorgi, F. 2013 Summer monsoon rainfall scenario over Bangladesh using a high-resolution AGCM. *Nat. Hazards* **69**, 793–807. https://doi.org/10.1007/s11069-013-0734-7.

Rajendran, K., Kitoh, A., Srinivasan, J., Mizuta, R. & Krishnan, R. 2012 Monsoon circulation interaction with Western Ghats orography under changing climate. *Theor. Appl. Climatol.* **110**, 555–571. https://doi.org/10.1007/s00704-012-0690-2.

Reggiani, P. & Rientjes, T. H. M. 2015 A reflection on the long-term water balance of the Upper Indus Basin. *Hydrol. Res.* **46**, 446–462. https://doi.org/10.2166/nh.2014.060.

Rounce, D. R., Hock, R. & Shean, D. E. 2020 Glacier mass change in high mountain Asia through 2100 using the open-source Python Glacier Evolution Model (PyGEM). *Front. Earth Sci.* **7**. https://doi.org/10.3389/feart.2019.00331.

Sanjay, J., Krishnan, R., Shrestha, A. B., Rajbhandari, R. & Ren, G.-Y. 2017 Downscaled climate change projections for the Hindu Kush Himalayan region using CORDEX South Asia regional climate models. *Adv. Clim. Change Res.* **8**, 185–198. https://doi.org/10.1016/j.accre.2017.08.003.

Sayama, T. 2015 *RRI User manual*.

Sayama, T., Ozawa, G., Kawakami, T., Nabesaka, S. & Fukami, K. 2012 Rainfall–runoff–inundation analysis of the 2010 Pakistan flood in the Kabul River basin. *Hydrol. Sci. J.* **57**, 298–312. https://doi.org/10.1080/02626667.2011.644245.

Shah, M. I., Khan, A., Akbar, T. A., Hassan, Q. K., Khan, A. J. & Dewan, A. 2020 Predicting hydrologic responses to climate changes in highly glacierized and mountainous region Upper Indus basin. *R. Soc. Open Sci.* **7**, 191957. https://doi.org/10.1098/rsos.191957.

Su, F., Zhang, L., Ou, T., Chen, D., Yao, T., Tong, K. & Qi, Y. 2016 Hydrological response to future climate changes for the major upstream river basins in the Tibetan Plateau. *Global Planet. Change* **136**, 82–95. https://doi.org/10.1016/j.gloplacha.2015.10.012.

Terink, W., Lutz, A. F., Simons, G. W. H., Immerzeel, W. W. & Droogers, P. 2015 SPHY v2.0: spatial processes in Hydrology. *Geosci. Model Dev.* **8**, 2009–2034. https://doi.org/10.5194/gmd-8-2009-2015.

Valéry, A., Andréassian, V. & Perrin, C. 2014 'As simple as possible but not simpler': what is useful in a temperature-based snow-accounting routine? Part 2 – sensitivity analysis of the Cemaneige snow accounting routine on 380 catchments. *J. Hydrol.* **517**, 1176–1187. https://doi.org/10.1016/j.jhydrol.2014.04.058.

Wester, P., Mishra, A., Mukherji, A. & Shrestha, A. B. 2019 *The Hindu Kush Himalaya Assessment*. Springer International Publishing, Cham. https://doi.org/10.1007/978-3-319-92288-1.

Yatagai, A., Kamiguchi, K., Arakawa, O., Hamada, A., Yasutomi, N. & Kitoh, A. 2012 APHRODITE: constructing a long-term daily gridded precipitation dataset for Asia based on a dense network of rain gauges. *Bull. Am. Meteorol. Soc.* **93**, 1401–1415. https://doi.org/10.1175/BAMS-D-11-00122.1.

First received 22 April 2022; accepted in revised form 1 August 2022. Available online 12 August 2022

Downloaded from http://iwaponline.com/jwcc/article-pdf/13/9/3416/1114580/jwc0133416.pdf
by KYOTO UNIVERSITY user